Research on negative ion-functional inorganic artificial stone

Chi Lei[1], Haijun Xu[2], Zhiguo Zhou[3], Hesong Hu[4], Xiaopeng Wu[5], Zhijie Zhang[6], Mingfeng Zhong[7]
[1, 2, 3]Yuanchuang New Materials and Technology Co., Ltd., Guangzhou, 510440, China
[4]Guangzhou Construction Co., Ltd., Guangzhou, 510030, China
[5, 6, 7]School of Materials Science and Engineering, South China University of Technology, Guangzhou, 510230, China
[2]Corresponding author
E-mail: [1]*413505720@qq.com*, [2]*2649727362@qq.com*, [3]*csu_zzhg@163.com*, [4]*39870229@qq.com*, [5]*810542875@qq.com*, [6]*imzhang@scut.edu.cn*, [7]*mfzhong@scut.edu.cn*

Received 11 February 2026; accepted 23 March 2026; published online 22 April 2026
DOI https://doi.org/10.21595/vp.2026.26114

75th International Conference on Vibroengineering in Trieste, Italy, April 13, 2026

Abstract. In architectural decoration, inorganic artificial stone has become a widely used material. However, it suffers from limited surface performance and functional simplicity. In this study, tourmaline was modified to enhance its negative-ion release capacity. The modified negative ion powder was used as a filler to prepare a negative ion-type UV curable coating (UVCC), which was then applied to the surface of artificial stone to obtain a negative ion-functional inorganic artificial stone. The results show that when 30 % by mass of CeO_2 is added to 1200-mesh tourmaline powder, the negative ion release capacity of the composite powder increases from 197 ions/cm^3 to 586 ions/cm^3. After heat treatment at 900 ℃ for 1 hour, the negative ion release capacity of the composite powder further rises to 828 ions/cm^3. When 15 % of the modified negative ion powder is incorporated into the basic UVCC formula, the prepared negative ion-type UVCC coating enables the artificial stone to achieve a negative ion release capacity of over 500 ions/cm^3, with a coating gloss higher than 90°, a hardness of 4 H, and an adhesion of grade 1. This work successfully improves both surface properties and health functionality, broadening the application potential of inorganic artificial stone.

Keywords: inorganic artificial stone, negative-ion function, tourmaline powder, rare earth doping, ultraviolet light curing coating.

1. Introduction

Artificial stone is inexpensive and durable, yet it is susceptible to corrosion and staining. Applying a protective surface coating can render it water-resistant, acid-proof, and easy to clean. Additionally, it enables the release of negative ions that are beneficial to health, which significantly broadens its potential applications.

Tourmaline, a trigonal borosilicate mineral, has the general structural formula $NaR_3Al_6[Si_6O_{18}][BO_3]_3(OH, F)_4$, where R = Mg, Li, Fe, Mn, or Al [1]. Due to its unique polar structure and complex chemical composition, natural tourmaline displays a persistent surface electric field, along with piezoelectric and pyroelectric properties [2]. This allows it to ionize surrounding water and oxygen molecules, thus generating negative ions. Apart from being beneficial to human health, negative air ions have bactericidal, air-purifying, and deodorizing effects, making tourmaline an ideal green and environmentally friendly material [3-5].

Although tourmaline is currently the primary raw material used as a negative-ion additive because of its excellent negative-ion performance, the chemical composition of tourmaline ore varies significantly across different mining regions, resulting in substantial disparities in negative-ion release capacity. Most commercial tourmaline powders exhibit relatively low negative-ion emission. The negative-ion performance of tourmaline can be improved through

several methods, including particle refinement, surface modification, and compounding with rare-earth oxides, carbon materials, and other substances [6-9].

UV-curable coatings (UVCC) offer advantages such as energy efficiency, environmental friendliness, and rapid curing, overcoming the drawbacks of solvent-based coatings (harmful to humans and polluting) and water-based coatings (inadequate film performance). After curing, UVCC films have high gloss, hardness, and wear resistance. Compared with thermal curing technologies, ultraviolet curing is more energy-efficient and productive, making it more suitable for large-scale industrial applications.

Therefore, to overcome the limitations of inorganic artificial stone, such as low surface gloss, poor acid resistance, and limited functionality, this study modifies tourmaline powder to enhance its negative-ion emission and formulates a negative-ion-type UV-curable coating for application on artificial stone surfaces. The resulting functional inorganic artificial stone achieves a negative-ion release exceeding 500 ions/cm^3, a coating gloss above 90°, a hardness of 4 H, and a Grade 1 adhesion rating, successfully integrating enhanced surface properties with a functional health-promoting feature.

2. Materials and methods

The primary materials included aluminate cement-based artificial stone, 1200-mesh tourmaline powder (Shenzhen Baohua Negative Ion Powder Co., Ltd.), cerium oxide (analytical grade, Shanghai Chemical Reagent Purchase and Supply Station), epoxy acrylate (EA) 621A-80, and polyester acrylate (PEA) P175D (both from Guangzhou Handong Trading Co., Ltd.).

Negative-ion release capacity was measured with a KEC-900 ion concentration tester (Japan) paired with an R2-104 recorder. X-ray diffraction (XRD) analysis was conducted on a D/max-IIIA diffractometer (Cu-Kα radiation, 40 kV, 100 mA, step 0.01°, range 5-90°). The chemical composition of the tourmaline powder was determined using a PW4400 X-ray fluorescence (XRF) spectrometer.

Coating pencil hardness was tested according to GB/T6739-2006, adhesion by the cross-cut method per GB/T9286-1998, and 60° gloss with an ETB-0686 gloss meter following GB9754-88. Surface wettability was evaluated via contact-angle measurement using a DSA100 droplet imaging system (KRÜSS, Germany; range 0-180°, accuracy ±0.1°).

3. Results and analysis

The 1200-mesh tourmaline powder used in this study exhibited a low initial negative ion release capacity, measuring only 197 ions/cm^3. XRD and XRF analyses were conducted to characterize its crystalline phase and chemical composition, and the corresponding results are presented in Fig. 1 and Table 1.

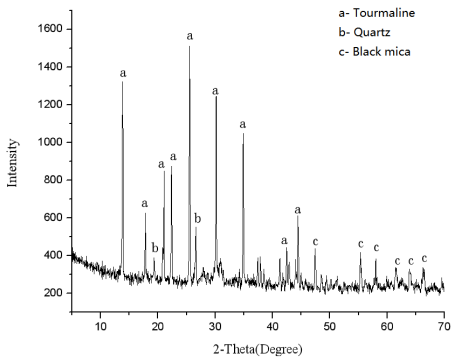

Fig. 1. XRD pattern of tourmaline powder

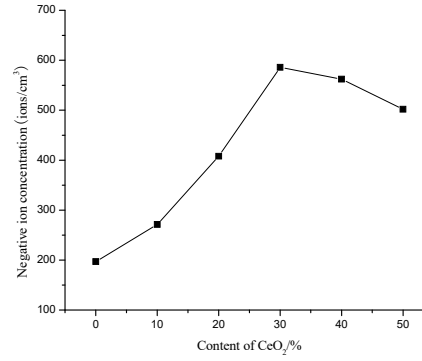

Fig. 2. Negative ion concentration of composite tourmaline powder

As shown in Fig. 1, the XRD pattern of the tourmaline powder displays distinct characteristic diffraction peaks of tourmaline, such as (220), (012), (122), and (042). Apart from the main tourmaline phase, peaks corresponding to associated minerals, including quartz and biotite, are also observed, indicating the presence of impurities in the raw powder.

Table 1. Chemical composition of tourmaline powders

Component / %	
SiO_2	46.943
Al_2O_3	18.439
Fe_2O_3	14.789
MgO	14.619
CaO	3.468
Na_2O	1.028
K_2O	0.237
MnO_2	0.169
TiO_2	0.143

As shown in Table 1, the tourmaline powder is primarily composed of SiO_2, Al_2O_3, Fe_2O_3, and MgO. The contents of Fe_2O_3 and MgO are similar, indicating that the powder belongs to the iron-magnesium tourmaline type. The Fe_2O_3/MgO ratio significantly influences its pyroelectric properties: a higher ratio corresponds to a more pronounced reduction in the pyroelectric coefficient, ultimately diminishing the negative-ion release capacity of the tourmaline.

Tourmaline powder can generate negative ions mainly due to the presence of a spontaneous electric field around the powder. The specific process of negative ion generation is as follows: when water molecules in the air enter the electric field space of tourmaline powder (generally a sphere with a radius of 10-15 μm), they are immediately ionized by the permanent electrodes, undergoing the following reactions: $H_2O \rightarrow OH^- + H^+$.

Since H^+ moves very fast (the mobility of H^+ is 1.8 times that of OH^-), it quickly moves to the negative pole of the permanent electrode, absorbs one electron, and becomes H_2, which escapes into the air. Meanwhile, OH^- combines with another water molecule to form $H_3O_2^-$ negative ions, namely:$2H^+ + 2e^- \rightarrow H_2\uparrow$; $OH^- + H_2O \rightarrow H_3O_2^-$.

The negative ion release capacity of raw tourmaline powder is low, which cannot meet the usage requirements. In this study, rare earth elements were added to tourmaline powder, and heat treatment was carried out to change its structure in order to observe the variation trend of the powder's negative ion release capacity. Ultimately, tourmaline-based negative ion functional powder with high negative ion release capacity was obtained.

CeO_2 accounting for 10 %, 20 %, 30 %, 40 %, and 50 % of the powder mass was added to the raw tourmaline powder, and composite powders were obtained after ball milling. The experimental results of the negative ion release capacity are shown in Fig. 2.

As shown in Fig. 2, incorporating an appropriate amount of CeO_2 into the raw tourmaline powder can effectively enhance its negative ion release capacity. At a CeO_2 content of 30 %, the negative ion emission increased from the initial 197 ions/cm^3 to 586 ions/cm^3. However, further increasing the CeO_2 content to 50 % led to a decline in performance, with the release capacity dropping to 502 ions/cm^3.

The enhancement mechanism can be attributed to the unique electronic structure of rare-earth elements, which have partially filled 4f orbitals, multiple energy levels, and high chemical activity. Their ability to lose electrons and undergo valence transitions, along with β-ray emission, can strengthen the spontaneous electric field and ionization capability of tourmaline, thereby promoting negative ion generation. However, when the rare-earth content exceeds 30 %, the proportion of active tourmaline per unit mass decreases, the rare-earth elements no longer fully contribute to field enhancement, resulting in weaker ionization and lower negative ion yield.

As illustrated in Fig. 3, incorporating an appropriate amount of CeO_2 into the raw tourmaline powder effectively enhances its negative ion release capacity. At a CeO_2 content of 30 %, the

negative ion emission increased from the initial 197 ions/cm^3 to 586 ions/cm^3. However, further increasing the CeO_2 content to 50 % resulted in a decline in performance, with the release capacity dropping to 502 ions/cm^3.

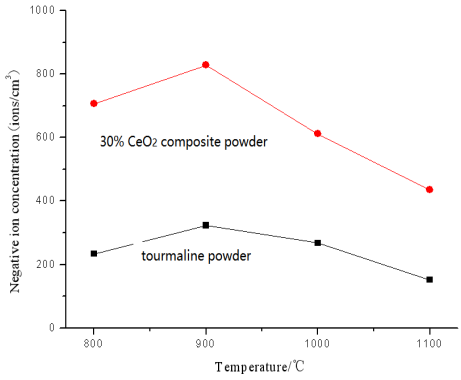

Fig. 3. Negative ion concentration of tourmaline powders with heat treatment

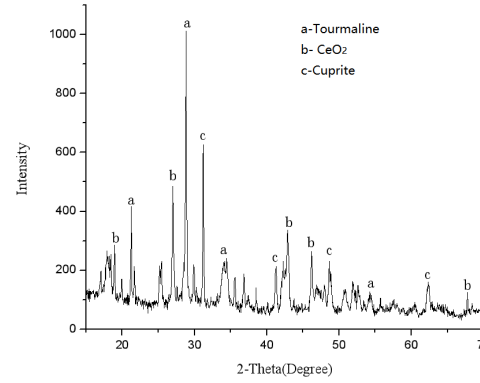

Fig. 4. XRD pattern of tourmaline powder with CeO_2 after heat treatment at 900 °C

After treatment, the powder turns reddish-brown. XRD in Fig. 4 confirms that the tourmaline structure remains with minor cuprite formation. Heat-induced oxidation of Fe^{2+} to Fe^{3+} shrinks the crystal lattice, enhancing spontaneous polarity and surface energy. Thermal treatment facilitates transitions of outer-shell electrons in rare-earth elements between different energy levels, increasing their activity and intensifying the decay-induced radiation energy [4]. Through these combined effects, the spontaneous electric field of the powder is strengthened, its ionization capacity is enhanced, and ultimately, the negative ion release performance is significantly improved.

Different amounts of modified tourmaline-based negative-ion powder were incorporated into the base UVCC formulation (EA: PEA = 3:2) to investigate the negative-ion release performance of the coating. During testing, the coating area (8×8 cm^2) and measurement distance (15 cm) were kept constant. After full curing, the negative-ion release capacity, gloss, adhesion, and hardness of the coated artificial stone were evaluated. The specific test results are summarized in Table 2.

Table 2. Negative ion concentration and coating properties of UVCC with different contents of negative ion powder

Content / %	5	10	15	20	25
Hardness	5 H	4 H	4 H	3 H	2 H
Adhesion (Grade)	1	1	1	3	5
Glossiness / 60°	97.5°	95.0°	93.7°	87.5°	65.9°
Negative ion release capacity / (ions/cm^3)	154	375	518	602	757

As shown in Table 2, the coating properties vary correspondingly with the negative-ion powder content. When the content is 5 %, the coating exhibits optimal hardness, adhesion, and gloss, but its negative-ion release capacity is insufficient for practical use. As the content increases, the hardness and gloss gradually decrease, while the negative-ion release capacity improves. At a content of 15 %, the negative-ion release reaches 518 ions/cm^3, and the coating maintains high hardness and gloss.

The inorganic artificial stone was surface-treated and then coated with a negative ion-type UVCC to prepare a negative ion-functional artificial stone. The content of modified composite negative ion powder in the negative ion-type UVCC was 15 %, the coating area was 8×8 cm^2, and after complete curing, the various properties of the artificial stone before and after coating were compared and tested.

As indicated in Table 3, coating the inorganic artificial stone with negative-ion UVCC

significantly enhances its surface properties. The gloss increases from 29.7° to 90.3°, resulting in a high-gloss surface. The coating also achieves a Grade 1 adhesion rating, and the negative-ion release capacity reaches 529 ions/cm^3, markedly improving both the appearance and functional performance of the artificial stone.

Table 3. Contrast test results of negative ion-functional inorganic artificial stone

Performance index	Before composite	After composite
Negative ion release capacity / (ions/cm^3)	0	529
Glossiness / 60°	29.7°	90.3°
Hardness	> 6 H	4 H
Adhesion (Grade)	–	1

To evaluate the acid resistance, a 10 mol/L sulfuric acid solution was applied to the stone surface before and after UVCC coating. After 24 hours, the acid was wiped off, and the surface corrosion condition was examined to assess acid resistance.

When the sulfuric acid solution was dropped onto the surface of the uncoated inorganic artificial stone, a large number of bubbles were generated, indicating a violent reaction between the sulfuric acid and calcium carbonate in the stone, producing CO_2 gas. In contrast, dropping the same concentration of sulfuric acid solution on the surface of the UVCC-coated artificial stone produced no bubbling.

As shown in Fig. 5(a), the surface of the uncoated stone appears uneven with substantial white corrosion products; whereas the coated surface (Fig. 5(b)) shows no obvious changes, with no coating peeling or blistering. These results demonstrate that the acid resistance of the inorganic artificial stone is significantly improved after coating.

To evaluate changes in surface hydrophobicity, the contact angles of the inorganic artificial stone before and after UVCC coating were measured. The results are presented in Fig. 5. As shown in Fig. 5, the contact angle of the surface of the inorganic artificial stone before coating is 24.8°, and it increases to 86.5° after UVCC coating.

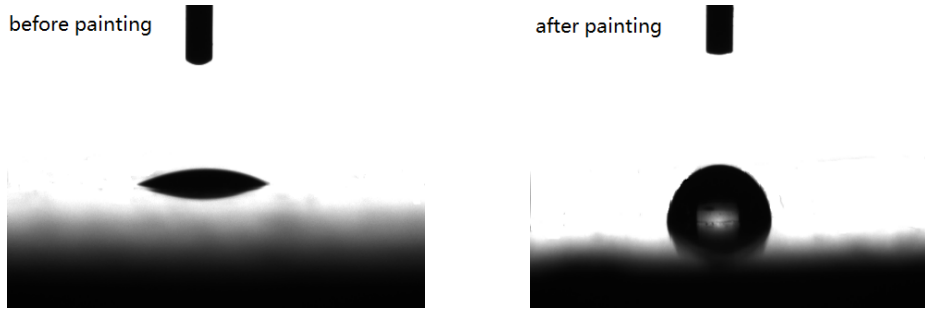

a) b)

Fig. 5. Contact angle of the surface of inorganic artificial stone.
Photo by Xiaopeng Wu in Guangzhou, 2024

4. Conclusions

In this study, raw tourmaline powder was modified to enhance its negative-ion release capacity, and a functional UV-curable coating was prepared using the modified composite negative-ion powder. Applying this coating onto the surface of inorganic artificial stone not only improved the stone's surface properties but also endowed it with negative-ion release functionality. By adding 30 wt% CeO_2 to 1200-mesh tourmaline powder, the negative-ion release capacity of the composite powder increased from 197 ions/cm^3 to 586 ions/cm^3. After heat treatment at 900 °C for 1 h, the release capacity further rose to 828 ions/cm^3. When 15 % of the modified composite negative-ion powder was incorporated into the UVCC formulation, the coated

inorganic artificial stone exhibited a negative-ion release capacity exceeding 500 ions/cm^3, along with a gloss > 90°, a hardness of 4 H, and Grade 1 adhesion. Moreover, the coating effectively improved the inherently poor acid resistance of the inorganic artificial stone and enhanced its stain resistance. The findings presented in this paper are expected to significantly broaden the application range and practical performance of artificial stone. The release amount of negative ions in the artificial stone with negative ion function may decline over a long period of use. This issue requires further investigation.

Acknowledgements

The research described in this paper was financially supported by the 2022 Science and Technology Innovation Plan Project of the Guangdong Provincial Department of Housing and Urban-Rural Development (Grant No. 2022-K25-534807) and the Science and Technology Planning Project of Guangzhou Municipal Construction Group Co., Ltd (Grant No. [2022]-KJ009).

Data availability

The datasets generated during and/or analyzed during the current study are available from the corresponding author on reasonable request.

Conflict of interest

The authors declare that they have no conflict of interest.

References

[1] J. Han, H. Chen, H. Xu, O. Nadeau, and C. Xu, "Identifying xenocrystic tourmaline in Himalayan leucogranites," *American Mineralogist*, Vol. 108, No. 7, pp. 1289–1297, Jul. 2023, https://doi.org/10.2138/am-2022-8615

[2] R. Shahrokhi, Y. Byun, H.-B. Moon, and J. Park, "A green approach to PFAS remediation: Mechanochemical degradation with natural piezoelectric tourmaline," *Journal of Hazardous Materials*, Vol. 502, p. 141040, Jan. 2026, https://doi.org/10.1016/j.jhazmat.2026.141040

[3] L. Zhao et al., "Exploring utilization of tourmaline in constructed wetlands to enhance nutrient reduction under fluoride stress: Performance and microbial mechanism," *Chemical Engineering Journal*, Vol. 522, p. 167482, Oct. 2025, https://doi.org/10.1016/j.cej.2025.167482

[4] Y. Liu, Y. Rui, B. Yu, L. Fu, G. Lu, and J. Liu, "Study on the negative oxygen ion release behavior and mechanism of tourmaline composites," *Materials Chemistry and Physics*, Vol. 313, p. 128779, Feb. 2024, https://doi.org/10.1016/j.matchemphys.2023.128779

[5] X. Wang et al., "Photocatalytic degradation of surface-coated tourmaline-titanium dioxide for self-cleaning of formaldehyde emitted from furniture," *Journal of Hazardous Materials*, Vol. 420, p. 126565, Oct. 2021, https://doi.org/10.1016/j.jhazmat.2021.126565

[6] P. Zhou et al., "Interfacial synergy-driven catalysis: Tourmaline supported Ni-NiAl2O4 catalyst for enhanced methane dry reforming activity," *Applied Surface Science*, Vol. 710, p. 163932, Nov. 2025, https://doi.org/10.1016/j.apsusc.2025.163932

[7] M. Han, Z. Liu, T. Zhang, M. Liu, and C. Li, "Preparation and formation mechanism study of tourmaline@nano-alumina composite filler," *Ceramics International*, Vol. 51, No. 11, pp. 13959–13967, May 2025, https://doi.org/10.1016/j.ceramint.2025.01.232

[8] C. Wang, Q. Chen, T. Guo, and Q. Li, "Environmental effects and enhancement mechanism of graphene/tourmaline composites," *Journal of Cleaner Production*, Vol. 262, p. 121313, Jul. 2020, https://doi.org/10.1016/j.jclepro.2020.121313

[9] Y. Xiong et al., "Efficient synergistic photocatalytic degradation by sunlight-driven natural tourmaline modified g-C3N4 interface electric field," *Separation and Purification Technology*, Vol. 361, p. 131496, Jul. 2025, https://doi.org/10.1016/j.seppur.2025.131496